Available online at www.sciencedirect.com
ScienceDirect
Ceramics International 35 (2009) 2633–2638
CERAMICS INTERNATIONAL
www.elsevier.com/locate/ceramint

Influence of nucleation agents on crystallization and machinability of mica glass–ceramics

Ping Wang [a], Liping Yu [a,*], Hanning Xiao [b], Yin Cheng [c], Shixun Lian [a]

[a] College of Chemistry and Chemical Engineering, Hunan Normal University, Changsha 410081, China
[b] College of Materials Science and Engineering, Hunan University, Changsha 410082, China
[c] Department of Materials Science and Engineering, Changsha University of Science and Technology, Changsha 410076, China

Received 10 October 2008; received in revised form 1 December 2008; accepted 27 February 2009
Available online 31 March 2009

Abstract

Effects of ZrO_2, La_2O_3, CeO_2, Yb_2O_3 and V_2O_5 on the crystallization kinetics, microstructure and mechanical properties of mica glass–ceramics were investigated by the differential scanning calorimetry (DSC), X-ray diffractometry (XRD), scanning electron microscopy (SEM) and microhardness tester. Results show that bulk crystallization can be obtained by introducing proper nucleation agents into the glass. Both Ozawa method and Kissinger method are suitable for analyzing the crystallization kinetics of mica glass–ceramic. The addition of nucleation agents has little influence on the value of n, keeping two-dimensional crystal growth mechanism. ZrO_2 and V_2O_5 are best nucleation agents in mica system. The increase of crystallization temperature is helpful for the increase of aspect ratio, and the microstructure of the glass–ceramics becomes interconnected, which contributes the improvement of the machinability of the glass–ceramics. Microhardness (H_v), cutting energy (μ^1) and machinability parameter (m) can be used for estimating the machinability of mica glass–ceramics.

Keywords: Mica glass–ceramics; Crystallization; Nucleation agent

1. Introduction

Mica glass–ceramics are widely used as mechanical, electrical and biomedical materials due to their unique machinability and good electrical properties. Unfortunately, the relatively poor mechanical performance limits their applications as structural material. Therefore, improving their mechanical properties has been attracted much interests [1–3]. Introducing stoichiometric Al_2O_3 and SiO_2 to mica glass–ceramic should be helpful for the separation of mullite, which is promising for improving mechanical properties of mica glass–ceramic by secondary phase toughening mechanism. In contrast, the addition of Al_2O_3 and SiO_2 would decrease the crystallization trend of the glass and consequently make it difficult to separate the phase of mullite [4]. Therefore, it is necessary to introduce some nucleation agents for improving the crystallization of mica glass–ceramics. Efficient nucleation of crystals from numerous centres would result in fine-grained microstructures and consequently high-strength [5,6].

ZrO_2 is an effective nucleation agent due to the characteristics of high electrovalency and cationic field strength, which facilitates the accumulation of glass matrix [7]. Also Yb_2O_3, La_2O_3, CeO_2 and V_2O_5 were reported as the effective nucleation agent for glass–ceramics [8–10]. Therefore, five nucleation agents ZrO_2, Yb_2O_3, La_2O_3, CeO_2 and V_2O_5 were introduced to investigate the influences of them on crystallization of mica glass–ceramics.

2. Experimental

Glass batches with the stoichiometric mica *vs.* mullite ratio of 7:3 were obtained by melting the reagents of Al_2O_3, $MgCO_3$, MgF_2, $ZrSiO_4$, K_2CO_3, SiO_2 and MgF_2 in an alumina crucible at 1500–1600 °C for 2 h, as shown in Table 1. The melts were cast into graphite molds to form 80 mm × 80 mm × 6 mm glass blocks and followed by slow cooling from 600 °C to room temperature at about 1 °C min^{-1} in order to relieve thermal stress.

* Corresponding author. Tel.: +86 731 8865345.
E-mail address: seaheart_yu@163.com (L. Yu).

0272-8842/$36.00
doi:10.1016/j.ceramint.2009.02.030

Table 1
Chemical compositions of glasses (wt%).

Sample No.	SiO_2	Al_2O_3	MgO	K_2O	MgF_2	ZrO_2	La_2O_3	CeO_2	Yb_2O_3	V_2O_5
1#	40.9	23.8	12.5	7.3	9.7	–	–	–	–	–
2#	40.9	23.8	12.5	7.3	9.7	5	–	–	–	–
3#	40.9	23.8	12.5	7.3	9.7	–	5	–	–	–
4#	40.9	23.8	12.5	7.3	9.7	–	–	5	–	–
5#	40.9	23.8	12.5	7.3	9.7	–	–	–	5	–
6#	40.9	23.8	12.5	7.3	9.7	–	–	–	–	5

Differential scanning calorimetry (DSC) was carried out on fine glass powders using a Netzsch STA-449C thermal analyzer with a heating rate of 10 °C min^{-1} in the temperature range from 10 °C to 1200 °C under air atmosphere. Crystalline phases were analyzed by a Rigaku D/max 2550VB+18kW diffractometer. Microstructure of the specimens was observed by JSM-5600LV scanning electron microscope. The machinability was evaluated by the drilling depth of the glass–ceramics within 30 s, using a 6 mm cermet bit in a drilling press of 50 kN at 500 rpm. Crystalized samples were ground and polished. Vickers hardness was performed on Leitz MM-6 microhardness tester with a pyramid-shaped diamond indenter (a load of 400 g for 5 s). Cutting energy (μ^1) at quasi-static state was given by [11,12]

$$\mu^1 = H_v^{2.25} \tag{1}$$

Machinability parameter m can be used to evaluate the effects of heat treatments as a function of temperature, time and H_v. Following equation indicates the relationship between hardness (H_v) and machinability parameter (m) [11,12]:

$$m = 0.643 - 0.122H_v \tag{2}$$

3. Results and discussion

3.1. Theoretical basis

Differential scanning calorimetry (DSC) is very effective for determining the kinetic parameters of glass crystallization under non-isothermal conditions [13–14]. The Johnson–Mehl–Avrami (JMA) equation is often used to describe the behavior of non-isothermal crystallization of glass:

$$-\ln\alpha(1-x) = kt^n \tag{3}$$

where x is the volume fraction of crystals precipitated in glass which can be estimated by the area of crystallization exothermal peak, n is a dimensionless factor depending on the nucleation process and growth morphology, k is the reaction rate constant.

After modified, Eq. (3) can be evaluated simply by Ozawa method [15]:

$$\ln\alpha = -\frac{E}{RT_p} + C_1 \tag{4}$$

where C_1 is a constant, α is the heating rate, E is the active energy of the crystallization process, T_p is the crystallization temperature. Therefore, activity energy E can be evaluated by the slope of $\ln\alpha - 1/T_p$. And the other modified method is Kissinger method [16]:

$$\ln\frac{T_p^2}{\alpha} = \frac{E}{RT_p} + \ln\frac{E}{R} - \ln \tag{5}$$

E can also be evaluated by the slope of $\ln(T_p^2/\alpha) - 1/T_p$. n can be estimated by Augis–Bennett equation [17]:

$$n = \frac{2.5}{\Delta T} \times \frac{RT_p^2}{E} \tag{6}$$

where ΔT is the interval temperature on the half height point of crystallization peak. $n = 1$, the crystallization mechanism belongs to surface crystallization; $n = 2$, the mechanism is two-dimensional growth; $n = 3$, that is three-dimensional growth.

3.2. Thermal stability

Fig. 1 shows DSC curves of glass samples at the heating rate of 10 °C min^{-1}. The glass transition temperature T_g, crystallization temperature T_p and the thermal stability index $\Delta T = T_p - T_g$ are listed in Table 2. The bigger difference ΔT indicates the more stable for glasses and lower tendency of crystallization.

As seen in Table 2, the addition of ZrO_2 caused 30 °C increase on T_g of base glass while 60 °C decreases on T_p. Consequently the thermal stability index ΔT decreases by 100 °C indicating an improvement on the crystallization of the

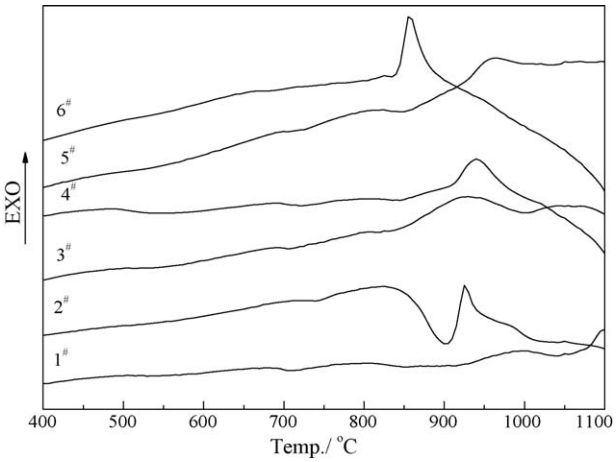

Fig. 1. DSC patterns of glass samples.

Table 2
Summary for physical parameters of glass samples with different nucleation agents.

Sample No.	T_g/°C	T_p/°C	$\Delta T = T_p - T_g$	n
1#	686.2	986.9	300.7	2.21
2#	716.5	925.4	208.9	2.51
3#	686.4	922.6	236.2	2.47
4#	708.0	940.9	232.9	2.31
5#	703.3	961.2	257.9	2.34
6#	667.1	856.7	189.6	2.49

glass. The addition of La_2O_3 has little effect on T_g and causes 64 °C decreases on crystallization temperature. By introducing CeO_2, T_g of sample 4# is 20 °C higher than that of sample 1#, while the crystallization temperature is 40 °C lower. The T_g of sample 5# with Yb_2O_3 is 17 °C higher than that of sample 1#, also the crystallization temperature decreases. Both T_g and T_p of sample 6# with V_2O_5 are lower than that of sample 1# and its thermal stability index is the smallest. According to the values of ΔT, the order of thermal stability of glass samples is $1^{\#} > 5^{\#} > 3^{\#} > 4^{\#} > 2^{\#} > 6^{\#}$.

3.3. Crystallization kinetics

Figs. 2–5 are Ozawa and Kissinger curves for the estimation of E. The plots of E with cationic field strength are shown in Fig. 6. The values of E estimated by two methods are different, but the tendency is similar. With the increase of cationic field strength, E decreases. E of the base glass is 459 kJ mol^{-1}. With the addition of ZrO_2, La_2O_3, CeO_2, Yb_2O_3 and V_2O_5, E decreases in different degree. The results show that the introduction of nucleation agents is beneficial to improve the crystallization ability of mica glass–ceramics. According to the values of E, the order of crystallization ability introduction of nucleation agents is $2^{\#} > 6^{\#} > 5^{\#} > 4^{\#} > 3^{\#} > 1^{\#}$, which is not consisted with the order of thermal stability.

The calculation results of n lie in the ranges of 2.21–2.51, indicating two-dimensional growth mechanism. This is consistent with the plate structure of mica crystal. The typical microstructures of mica glass–ceramics are shown in Fig. 7

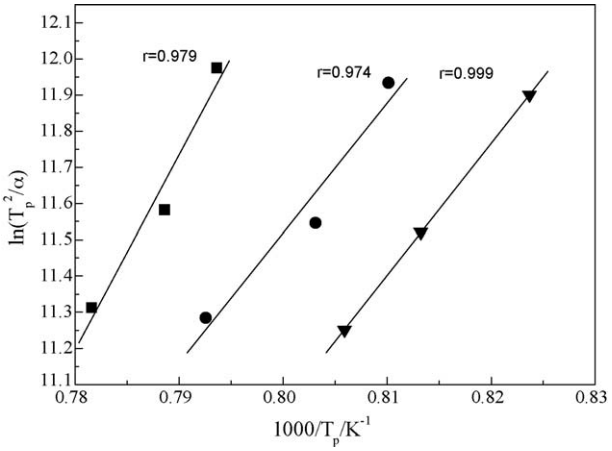

Fig. 2. Kissinger plot ($\ln(T_p^2/\alpha)$ *vs.* $1/T_p$) for determination of E: (■) sample 1#; (▼) sample 4#; (●) sample 5.

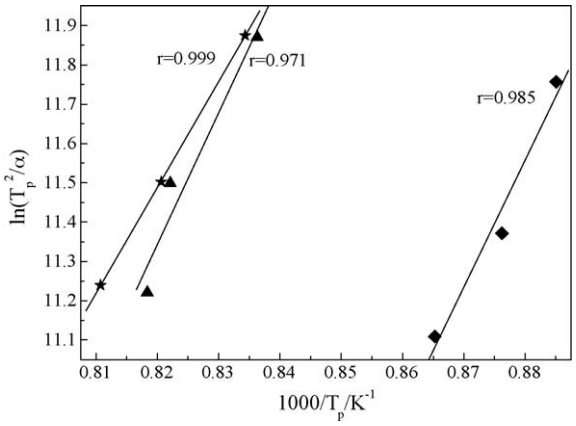

Fig. 3. Kissinger plot ($\ln(T_p^2/\alpha)$ *vs.* $1/T_p$) for determination of E: (★) sample 2#; (▲) sample 3#; (◆) sample 6.

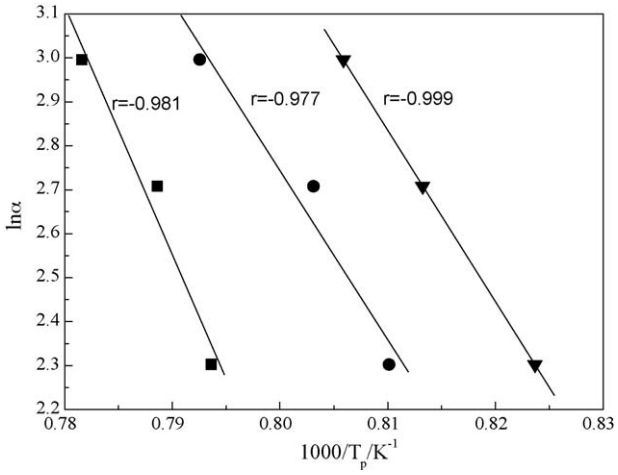

Fig. 4. Ozawa plot ($\ln \alpha$ *vs.* $1/T_p$) for determination of E: (■) sample 1#; (▼) sample 4#; (●) sample 5.

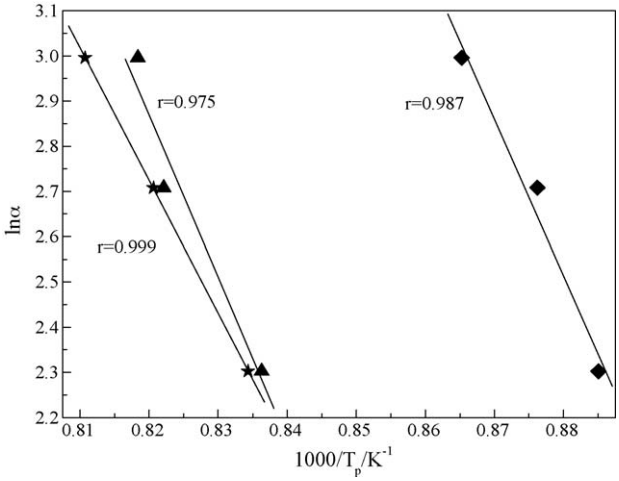

Fig. 5. Ozawa plot ($\ln \alpha$ *vs.* $1/T_p$) for determination of E: (★) sample 2#; (▲) sample 3#; (◆) sample 6.

3.4. Crystallization mechanism

The cation radius (r) and cation field strength (Z/r^2) of nucleation agents are listed in Table 3. The cationic field

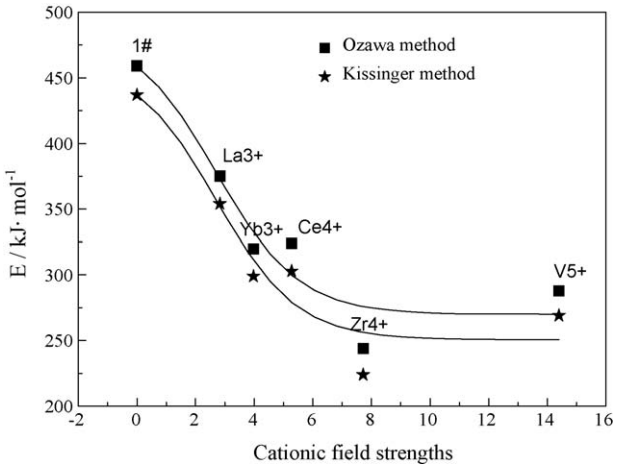

Fig. 6. The effect of cantionic field strength of different samples on activation energy of the crystallization process.

strength is the ability of a cation's effective force in attracting anions [18,19]. Glass transition temperatures increase linearly with increasing cation field strength of the rare earth modifiers in Ln–Si–Al–O–N glass system (Ln = Ce, Nd, Sm, Eu, Dy, Ho and Er) [20]. In this work, all samples except sample $1^{\#}$ and $6^{\#}$ are consistent with this change trend.

ZrO_2 can improve the nucleation and crystallization of mica glass–ceramic significantly in this work. The sample without nucleation agent (sample $1^{\#}$) is only surface crystallization after reheated at 1100 °C for 2 h owing to the high value of E. By introducing 5 wt% ZrO_2 (sample $2^{\#}$), the crystallization of the glass is greatly improved as seen in Fig. 7a and b. Bulk crystallization is observed after reheated at 1100 °C for 2 h.

La^{3+} usually lies at the interspaces of glass network owing to its big cation radius. E of glass $3^{\#}$ with La_2O_3 is relatively high, thereby the effect of La^{3+} on the nucleation and crystallization of the glass system is weaker than the other cations. However, the big cation radius of La^{3+} can enhance the difficulty of ion mobility and depress the growth of crystals [9], resulting in the fine particles as shown in Fig. 7c.

CeO_2 can be decomposed and release oxygen following the reaction equation:

$$2CeO_2 \overset{1400\,^{\circ}C}{\longrightarrow} Ce_2O_3 + [O]\uparrow$$

The release of oxygen is helpful for the clarification of melting process. According to Table 2, the addition of CeO_2 increases the nucleation temperature of the base glass as the strong accumulation of Ce^{4+} ($Z/r^2 = 5.28$).

Compared with La^{3+}, Yb^{3+} has smaller cation radius and higher cationic field strength, which is beneficial to the accumulation of non-bridge oxygen and ion mobility. Therefore Yb_2O_3 is more effective on improving the crystallization of mica glass–ceramics.

V_2O_5 can act as a glass former and has lower melting temperature. The radius of V^{5+} is littler bigger than that of Si^{4+} in [SiO_4] units, while its electron charge is higher than Si^{4+}. Usually the addition of V_2O_5 trends to phase separation, improving the nucleation and crystallization of the glass. From Fig. 7d, the layer mica crystals are observed and the aspect ratio

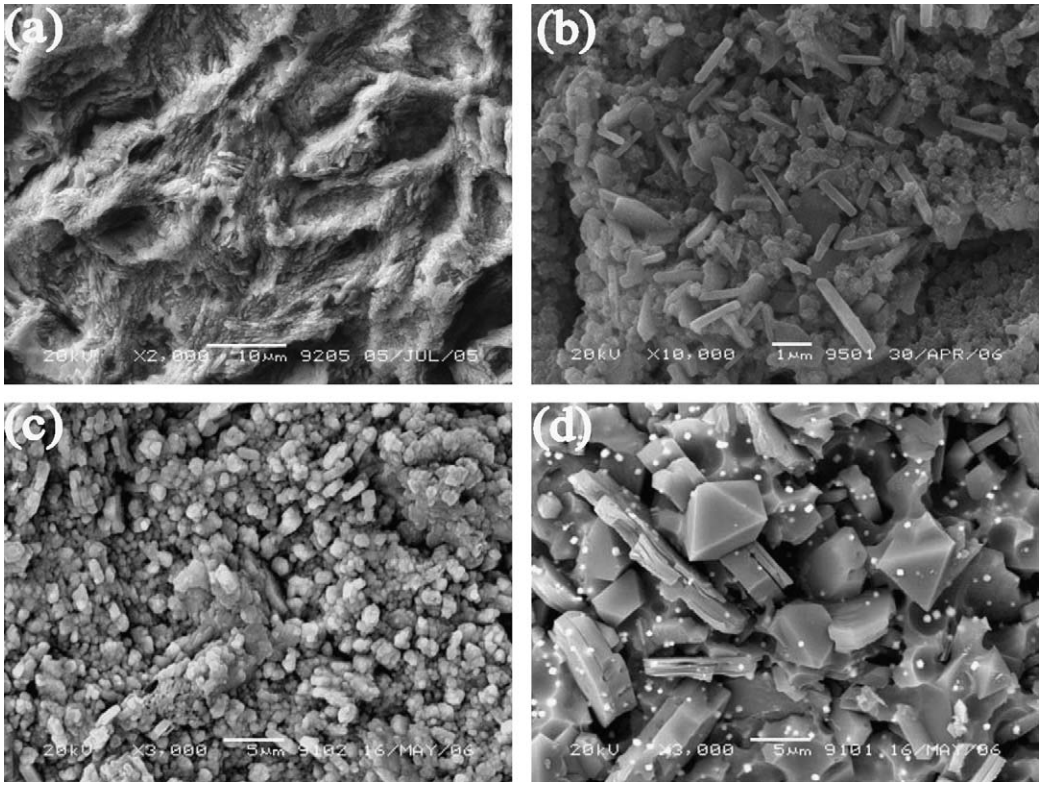

Fig. 7. SEM micrographs of glass samples reheated at 1100 °C for 2 h: (a) $1^{\#}$; (b) $2^{\#}$; (c) $3^{\#}$; (d) $6^{\#}$.

Table 3
Summary of ionic radius and electronic field intensity.

Ionic	Ionic radius/$\times 10^{-12}$ m	Cationic field strengths/Å^{-2}
Zr^{4+}	72	7.72
La^{3+}	103.2	2.83
Er^{3+}	89	3.79
Ce^{3+}	101	2.94
Ce^{4+}	87	5.28
Yb^{2+}	102	1.92
Yb^{3+}	86.8	3.98
V^{5+}	59	14.4

of mica crystal lies in the range of 6–10, forming an interconnected microstructure.

3.5. XRD analysis

Fig. 8 shows the XRD patterns of the glass–ceramics reheated at 1100 °C for 2 h. Sample 1# is only surface crystallized and its major phases are flurophlogopite and cordierite. The addition of ZrO_2, La_2O_3, CeO_2, Yb_2O_3 and V_2O_5 depressed the precipitation of cordierite, which is not beneficial to machinability of specimens [21]. Except flurophlogopite, a small amount of monoclinic zirconia, clinohumite, Al_2La, CeO_2, Yb_2O_3, VO_2 and V_2O_3 are respectively observed in glass–ceramics 2#, 3#, 4#, 5#, and 6#. The XRD results indicate that the oxides have limited solubility in the glass and promoted the crystallization of heterogeneous nucleation.

3.6. Mechanical properties

Table 4 shows machining properties of the samples reheated at 1100 °C and 1200 °C for 2 h. According to Table 4, glass–ceramic 1# has the lowest H_v value after reheated at 1100 °C for 2 h, but it has not machinability as it is only surface crystallization. After drilling out the surface layer, the inner glass is responsible for the fracture. Glass–ceramic 2# has the lowest H_v value except sample 1# after reheated at 1100 °C for 2 h and machinability parameter (m) is positive, indicating that glass–ceramic 2# has good machinability. With reheated temperature increasing, microhardness values of glass–ceramic 3# to 6# generally decrease. Glass–ceramic 6# shows a distinct minimum microhardness value (H_v 474 MPa) reheated at 1200 °C for 2 h, which suggests a highly machinability. The result is confirmed by the drilling depth data. The calculated results of cutting energy (μ^1) and machinability parameter (m) are also listed in Table 4. The lower the μ^1 value, the better the machinablity. The higher machinability parameter (m) values and lower cutting energy (μ^1) values are also indicating a highly machinable crystal microstructure, which has higher aspect ratio.

Table 4
Machining parameters of glass sample reheated at 1200 °C for 2 h.

Sample No.	Reheating temperature/°C	H_v/MPa	μ^1/J mm^{-3}	m
1#	1100	441	26.93	0.12
	1200	642	62.69	−0.12
2#	1100	530	40.73	0.01
	1200	824	109.9	−0.34
3#	1100	719	80.89	−0.22
	1200	514	38.01	0.03
4#	1100	613	56.50	−0.09
	1200	504	36.37	0.04
5#	1100	582	50.27	−0.05
	1200	527	40.21	−0.01
6#	1100	610	55.88	−0.09
	1200	474	31.68	0.08

The drilling depths of glass–ceramics are shown in Fig. 9. Sample 6# reheated at 1200 °C for 2 h has the largest drilling depth (5.05 mm), which is consistent with the results of microhardness, cutting energy (μ^1) and machinability parameter (m).

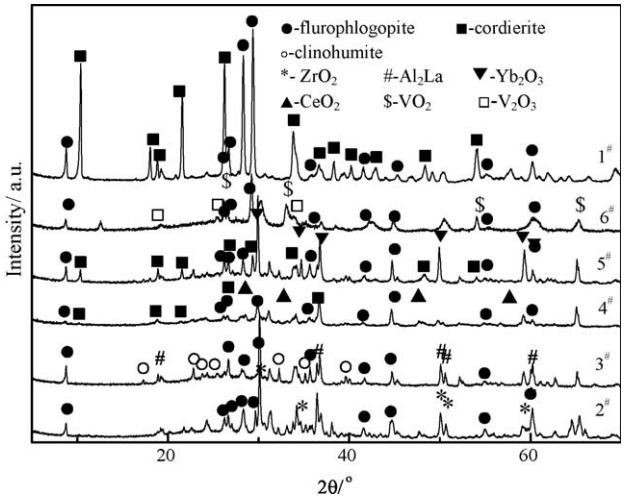

Fig. 8. XRD patterns of glass samples reheated at 1100 °C for 2 h.

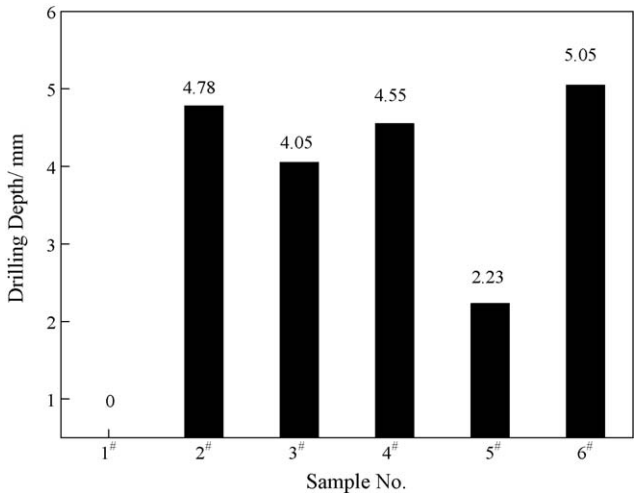

Fig. 9. The drilling depth of different samples.

4. Conclusions

(1) Bulk crystallization can be obtained by introducing ZrO_2, La_2O_3, CeO_2, Yb_2O_3 and V_2O_5 to mica glass–ceramics. The subsequence of improving crystallization of mica glass–ceramic is $ZrO_2 > V_2O_5 > Yb_2O_3 > CeO_2 > La_2O_3$.

(2) The values of activation energy E estimated by Ozawa method and Kissinger method are different, while its change trends are similar. Both the methods are proper for analyzing the crystallization kinetics of mica glass–ceramic. The additions of nucleation agents have little influence on the values of n, keeping two-dimensional crystal growth mechanism.

(3) The bigger the cationic field strength of nucleation agent, the smaller the activation energy of the glass. When cationic field strength is beyond the eight, the activation energy changes little.

(4) The increase of crystallization temperature is helpful for the increase of aspect ratio, which contributes for the machinability of the glass–ceramics. Microhardness (H_v), cutting energy (μ^1) and machinability parameter (m) can be used for estimating the machinability of glass–ceramics.

Acknowledgements

This work is supported by Scientific Research Fund of Hunan Provincial Education Department (No. 07C580) and the Scientific Research Fund of Hunan Normal University (No. 23040612).

References

[1] S. Habelitz, G. Carl, C. Rüssel, Processing microstructure and mechanical properties of extruded mica glass–ceramics, Mater. Sci. Eng. A 307 (2001) 1–14.
[2] S. Habelitz, C. Rüssel, S. Thiel, Mechanical properties of oriented mica glass ceramics, J. Non-Cryst. Solids 220 (1997) 291–298.
[3] T. Höche, S. Habelitz, I. Khodos, Origin of fluorophlogopite morphology in mica glass–ceramics of the system SiO_2–Al_2O_3–MgO–K_2O–Na_2O–F_2, J. Cryst. Growth 192 (1998) 185–195.
[4] L.P. Yu, H.N. Xiao, C. Yin, Microhardness and machinability of fluorphlogopite-mullite glass–ceramics, Key Eng. Mater. 353–358 (2007) 1576–1579.
[5] Uno Tomoko, Kosuga Toshihiro, Shin Nakayama, Microstructure of mica-based nanocomposite glass–ceramics, J. Am. Ceram. Soc. 76 (2) (1993) 539–541.
[6] D.U. Tulyaganov, S. Agathopoulos, H.R. Fernandes, Preparation and crystallization of glasses in the system tetrasilicic mica–fluorapatite–diopside, J. Eur. Ceram. Soc. 24 (2004) 3521–3528.
[7] P. Vomacka, O. Babushkin, R. Warren, Zirconia as a nucleating agent in a yttria–alumina–silica glass, J. Eur. Ceram. Soc. 15 (1995) 1111–1117.
[8] Naoki Kondo, Yoshikazu Suzuki, Tatsuya Miyajima, High-temperature mechanical properties of sinter-forged silicon nitride with ytterbia additive, J. Eur. Cer. Soc. 23 (2003) 809–815.
[9] Y. Zhang, A.L. Ding, P.S. Qiu, Effect of La content on characterization of PLZT ceramics, J. Mater. Sci. Eng. B 99 (2003) 360–362.
[10] P. Alizadeh, V.K. Marghussian, Effect of nucleating agents on the crystallization behaviour and microstructure of SiO_2–CaO–MgO (Na_2O) glass–ceramics, J. Eur. Ceram. Soc. 20 (6) (2000) 775–782.
[11] D.S. Baik, K.S. No, J.S. Chun, Effect of the aspect ratio of mica crystal and crystallinity on the microhardness and machinability of mica glass–ceramics, J. Mater. Proc. Technol. 67 (1997) 50–54.
[12] D.S. Baik, K.S. No, J.S. Chun, A comparative evaluation method of machinability of mica-based glass–ceramics, J. Mater. Sci. 30 (7) (1995) 1801–1806.
[13] H. Shao, K.M. Liang, F. Peng, Crystallization kinetics of MgO–Al_2O_3–SiO_2 glass–ceramics, Ceram. Int. 30 (6) (2004) 927–930.
[14] A.M. Hu, M. Li, D.L. Mao, Growth behavior, morphology and properties of lithium aluminosilicate glass ceramics with different amount of CaO, MgO and TiO_2 additive, Ceram. Int. 34 (2008) 1393–1397.
[15] T. Ozawa, Kinetics of non-isothermal crystallization, Polymer 12 (3) (1971) 150–158.
[16] H.E. Kissinger, Variation of peak temperature with heating rate in differential thermal analysis, J. Res. Natl. Bur. Stand. 57 (1956) 217–221.
[17] A. Augisj, E. Bennett, Calculation of Avrami parameters for heterogenous solids state reactions using a modification of the Kissinger method, J. Therm. Anal. 13 (1978) 283–292.
[18] W. Vogel, Structure and Crystallization Behavior of Glasses, Pergamon Press, Oxford, 1971.
[19] W. Vogel, Chemistry of Glass, the American Ceramic Society, Columbus, OH, 1985.
[20] R. Ramesh, E. Nestor, M.J. Pomeroy, S. Hampshire, Formation of Ln–Si–Al–O–N glasses and their properties, J. Eur. Ceram. Soc. 17 (15–16) (1997) 1933–1939.
[21] J. Henry, R.G. Hill, The influence of lithia content on the properties of fluorphlogopite glass–ceramics. II. Microstructure hardness and machinability, J. Non-Cryst. Solids 319 (2003) 13–30.